Supporting Information

Carbazole-Imidazole Synergy for Discriminative BSA Sensing and Self-Assembled Organogel

Dharmendra Adak,[a] Sulekha Kumari Pandit,[a] Rajan Kumar,[b] Abhishek Rameshchandra Tiwari,[a] Gopal Das,*[a] and Ammathnadu Sudhakar Achalkumar*[a,c]

[a]*Department of Chemistry,*
Indian Institute of Technology Guwahati, Guwahati, 781039, Assam, India.

[b]*Centre for Nanotechnology, Indian Institute of Technology Guwahati, Guwahati, Assam 781039, India*

[c]*Centre for Sustainable Polymers, Indian Institute of Technology Guwahati, Guwahati, 781039, Assam, India.*

Email addresses: achalkumar@iitg.ac.in; gdas@iitg.ac.in

Table of contents

Serial number	Contents	Page numbers
1	Materials and methods	S2-S3
2	Experimental section	S3-S4
3	NMR spectra	S4-S6
4	MALDI-TOF mass spectra	S7
5	Infrared spectra	S8
6	Thermogravimetric analysis and Differential scanning calorimetry	S9
7	Gel properties	S9-S10
8	Photophysical properties	S11-S16
9	Molecular docking	S16
10	References	S16

1. Materials and methods

Commercially available chemicals were used without further purification; solvents were dried according to standard procedures. Chromatography was carried out using either silica gel (100-200 mesh) or neutral aluminum oxide. For thin-layer chromatography, aluminum sheets pre-coated with silica gel were employed. IR spectra were acquired at room temperature using a PerkinElmer IR spectrometer (PerkinElmer UATR TWO). The spectral positions are reported in wave number (cm^{-1}) units. NMR spectra were recorded using a 400 MHz Nuclear Magnetic Resonance (NMR) Spectrometer (Make: Bruker, Model: AVANCE III HD). For ^{1}H NMR spectra, the chemical shifts are reported in ppm relative to TMS as an internal standard. Coupling constants are given in Hz. Mass spectra were obtained using a MALDI-TOF mass spectrometer (Matrix Assisted Laser Desorption Ionization- Time of Flight, Make: BRUKER Model: AUTOFLEX SPEED) with α-Cyano-4-hydroxycinnamic acid as a matrix. The transition temperatures and associated enthalpy changes were determined by a differential scanning calorimeter (Mettler Toledo DSC1) under a nitrogen atmosphere. The transition temperatures and associated enthalpy changes were determined by a differential scanning calorimeter (Mettler Toledo DSC1) under a nitrogen atmosphere. The transition temperatures obtained from calorimetric measurements of the first heating and cooling cycles, conducted at a rate of 5 °C/min, are tabulated. Thermogravimetric analysis (TGA) was performed using a thermogravimetric analyzer (Mettler Toledo, model TG/SDTA 851 e) under a nitrogen flow at a heating rate of 10 °C/min. Rheological studies were conducted using Anton Paar Rheocampus

MCR 102. The UV-Visible absorption spectra were archived on a Perkin-Elmer Lamda-365 + UV-Vis spectrophotometer using 10 mm path length quartz cuvettes in 250-600 nm wavelengths. Baseline correction was applied for all spectra. A fluorescence emission study was carried out using a Horiba Fluoromax-4 spectrofluorometer equipped with a xenon lamp source using a path length of 1 cm of quartz cuvettes having a slit width of 5 nm at 298 K. All readings were recorded in HPLC-grade solvent. The emission spectra of **CZDIM** were recorded. The excitation wavelength (λ_{ex} = 395 nm) and emission wavelength (λ_{em} = 410-700 nm) were used to record the fluorescence spectra at (298 K).

2. Experimental section

2.1. Synthetic scheme

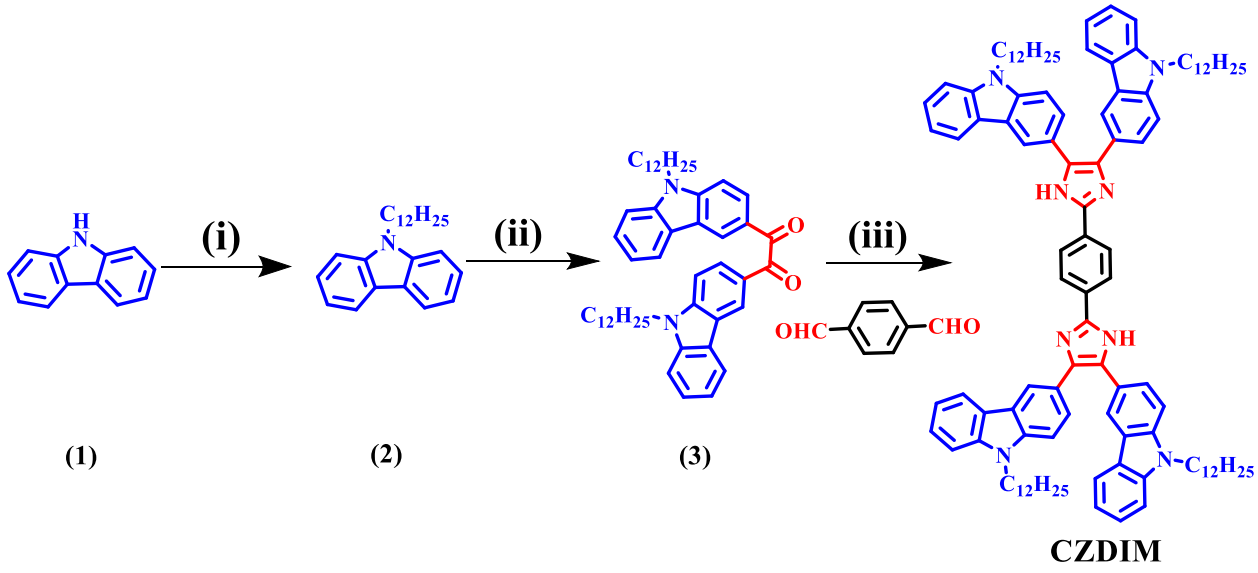

Reagent and conditions: (i) $C_{12}H_{25}Br$, DMF, KOH, RT, 18 h, 85%; (ii) 1,2-dichloromethane, oxalyl chloride, anhydrous $AlCl_3$, 0 °C (30 min), RT, 57%; (iii) NH_4OAc, CH_3COOH, 155 °C, MW, 10 min, 75-80%.

2.2. Synthetic procedure

The synthesis of compound **2** has been carried out according to the literature-reported method.[S1]

Procedure for synthesis of compound 3[S2]

To a 250 ml two-necked dried round-bottom flask (RB) under argon atmosphere containing the solution of 9-dodecyl-9H-carbazole (6.0 g, 17.88 mmol, 1.0 equiv.) in 1,2-dichloromethane (80 mL), was added oxalyl chloride (0.92 mL, 10.73 mmol, 0.6 equiv.) by syringe at 0 °C. The reaction mixture was retained at 0 °C for 10 min, and then anhydrous $AlCl_3$ (1.19 g, 9.09 mmol, 0.5 equiv.) was added. After 30 minutes at 0°C, the reaction mixture was allowed to reach room temperature and was kept overnight. The reaction mixture was then poured into a 100 mL HCl (1M) solution. The organic layer was then extracted twice with dichloromethane (DCM), dried

with anhydrous sodium sulphate, and concentrated. This crude product was purified using column chromatography with silica gel, eluting with 50% DCM-hexane to obtain the pure product. Removal of solvent yielded the product **3**.

Compound 3: R_f = 0.75 (10% EtOAc-Hexane); white color solid, yield: 57 %; IR: νmax in cm^{-1}: 3059, 2919, 2854, 1659, 1590, 1465, 1327, 1122, 721; ^{1}H NMR (400 MHz, $CDCl_3$), δ (ppm): 8.804-8.800 (d, *J* = 1.6 Hz, 2H, 2Ar**H**), 8.227-8.202 (dd, *J* = 8.8 Hz, 2H, 2Ar**H**), 8.116-8.096 (d, *J* = 8.0 Hz, 2H, 2Ar**H**), 7.528-7.427 (m, 6H, 6Ar**H**), 7.303-7.267 (t, *J* = 7.6 Hz, 2H, 2Ar**H**), 4.339-4.303 (t, *J* = 7.2 Hz, 4H, 2NC**H₂**), 1.893-1.858 (t, *J* = 6.8 Hz, 4H, 2NCH$_2$C**H₂**), 1.338-1.229 (m, 36H, 18**CH₂**), 0.888-0.854 (t, *J* = 6.8 Hz, 6H, 2**CH₃**). ^{13}C NMR (150MHz, $CDCl_3$), δ (ppm): 195.202, 144.134, 141.202, 127.787, 126.722, 124.889, 124.119, 123.119, 123.071, 120.936, 120.382, 109.384, 108.938, 43.449, 31.903, 29.585-28.934 (multi carbons in alkyl chain), 27.250, 22.686, 14.121. MALDI-TOF mass calculated for $C_{50}H_{64}N_2O_2$ ($M+H^+$): 725.0700, found: 725.0701.

Procedure for synthesis of CZDIM[S3]

Compound **3** (2.05 equiv.), terephthaldehyde (1.0 equiv.), and ammonium acetate (15 equiv.) were put together and dissolved in 3.0 mL of acetic acid in a 10 mL reaction vial containing a magnetic stir bar. The reaction vessel was heated in the microwave reactor cavity for 5 min at 155 °C, after which the vessel was cooled to room temperature. The reaction mixture was washed with distilled water, and a yellow precipitate was collected by filtration. The crude product was purified by column chromatography on alumina and dried with a vacuum pump to afford the product **CZDIM** as a yellow solid.

CZDIM: R_f = 0.41 (30% EtOAc-Hexane); yellow color solid, yield: 75 %; IR: νmax in cm^{-1}: 3468, 2918, 2849, 1599, 1467, 1317, 1146, 811, 743; ^{1}H NMR (400 MHz, $CDCl_3$), δ (ppm): 8.231 (s, broad, 4H, 4Ar**H**), 8.010 (s, broad, 4H, 4Ar**H)**, 7.855 (s, broad, 4H, 4Ar**H**), 7.537 (s, broad, 4H, 4Ar**H**), 7.377 (s, broad, 4H, 4Ar**H**), 7.310 (s, broad, 4H, 4Ar**H**), 7.079 (s, broad, 8H, 8Ar**H**), 4.074 (s, broad, 8H, 4NC**H₂**), 1.732 (s, broad, 8H, 4NCH$_2$C**H₂**CH$_2$), 1.263-1.196 (m, 72H, 36C**H₂**), 0.877-0.850 (t, *J* = 5.2 Hz, 12H, 4C**H₃**), 2N**H** protons not observed due to rapid exchange; ^{13}C NMR (150MHz, $CDCl_3$), δ (ppm): 140.635, 139.659, 126.308, 125.907, 125.441, 122.989, 122.853, 120.608, 119.811, 118.735, 108.563, 43.026, 31.930, 29.634-28.942 (multi carbons in alkyl chain), 27.303, 22.699, 14.129. MALDI-TOF mass calculated for $C_{108}H_{134}N_8$ ($M+H^+$): 1544.3200, found: 1544.3201.

3. NMR spectra

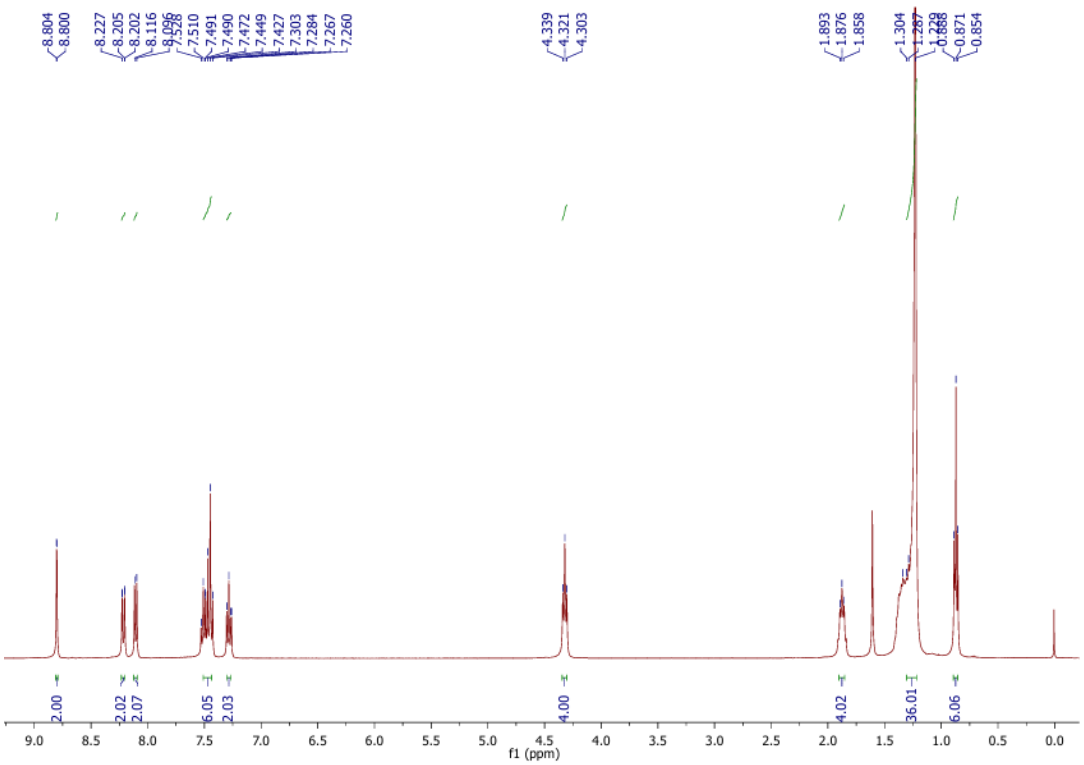

Figure S1 ^{1}H NMR (400 MHz) spectra of compound **3** in $CDCl_3$.

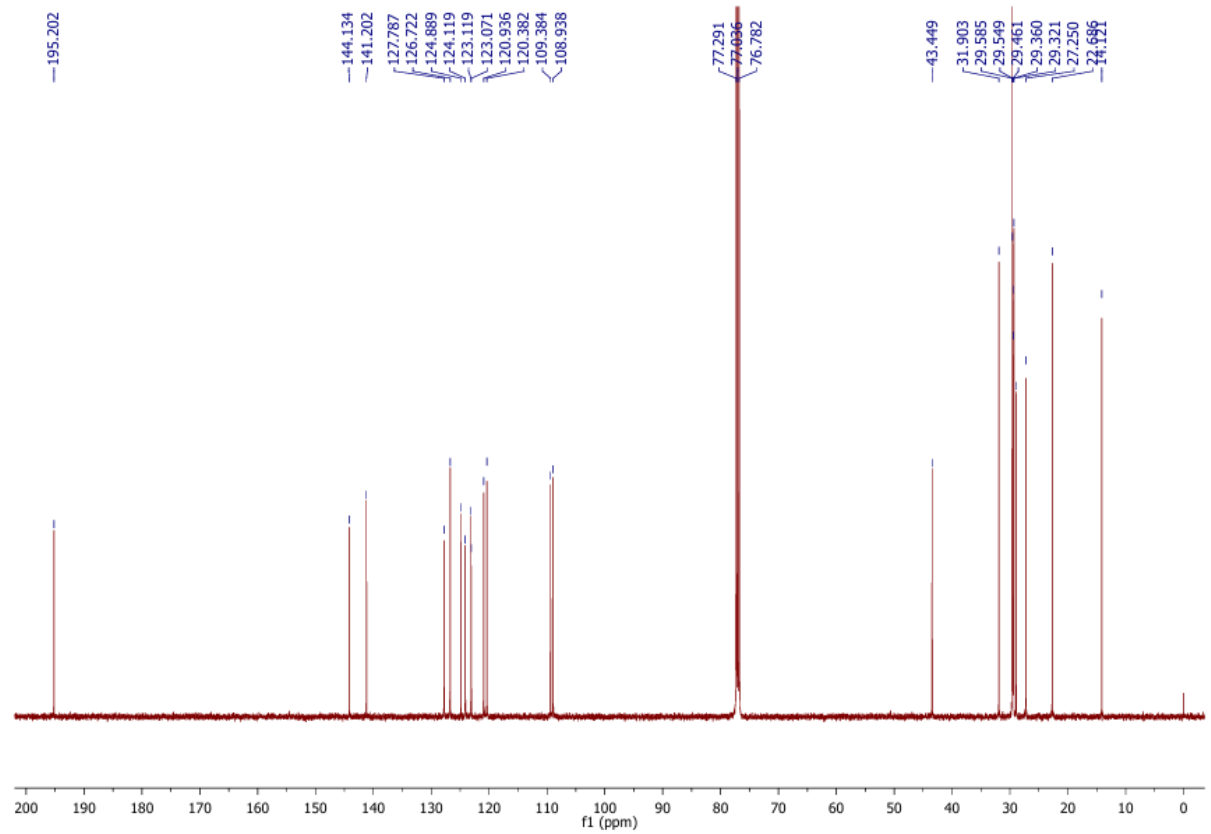

Figure S2 ^{13}C NMR (150 MHz) spectra of compound **3** in $CDCl_3$.

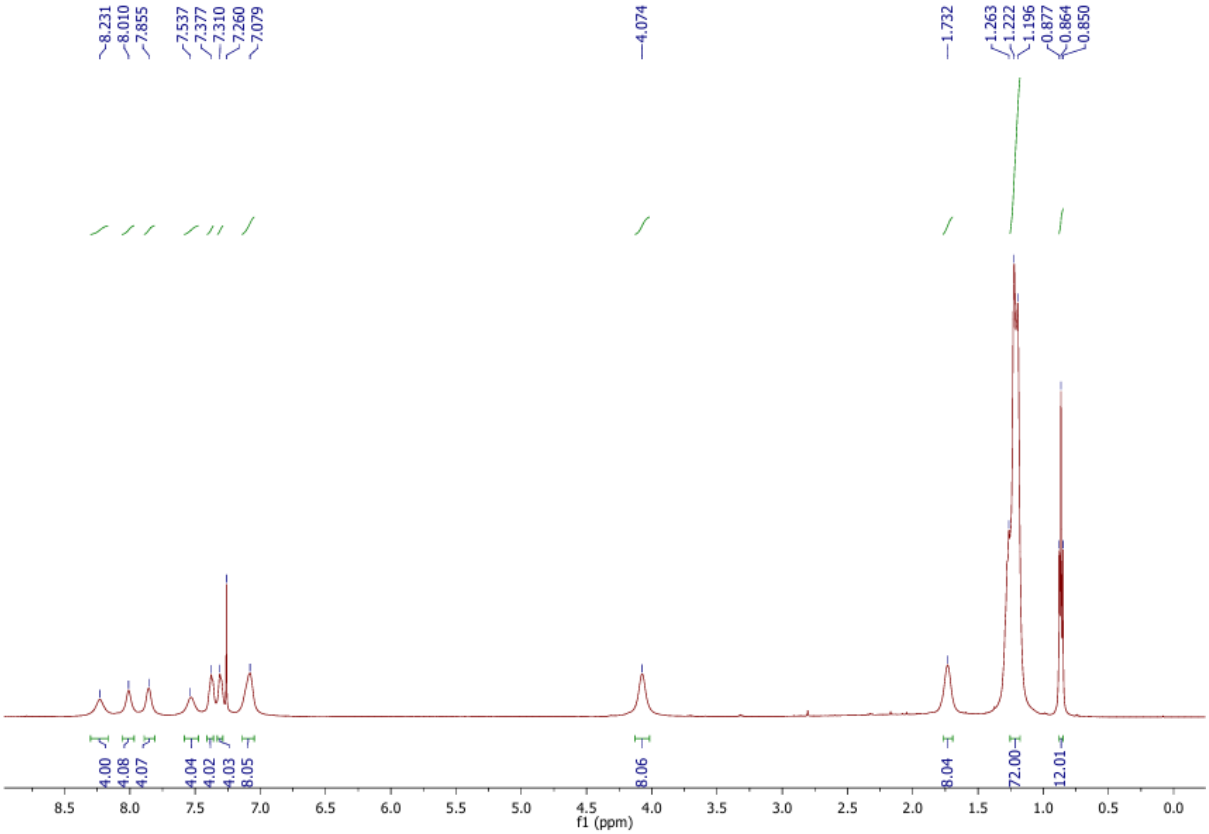

Figure S3 ^{1}H NMR (400 MHz) spectra of **CZDIM** in $CDCl_3$.

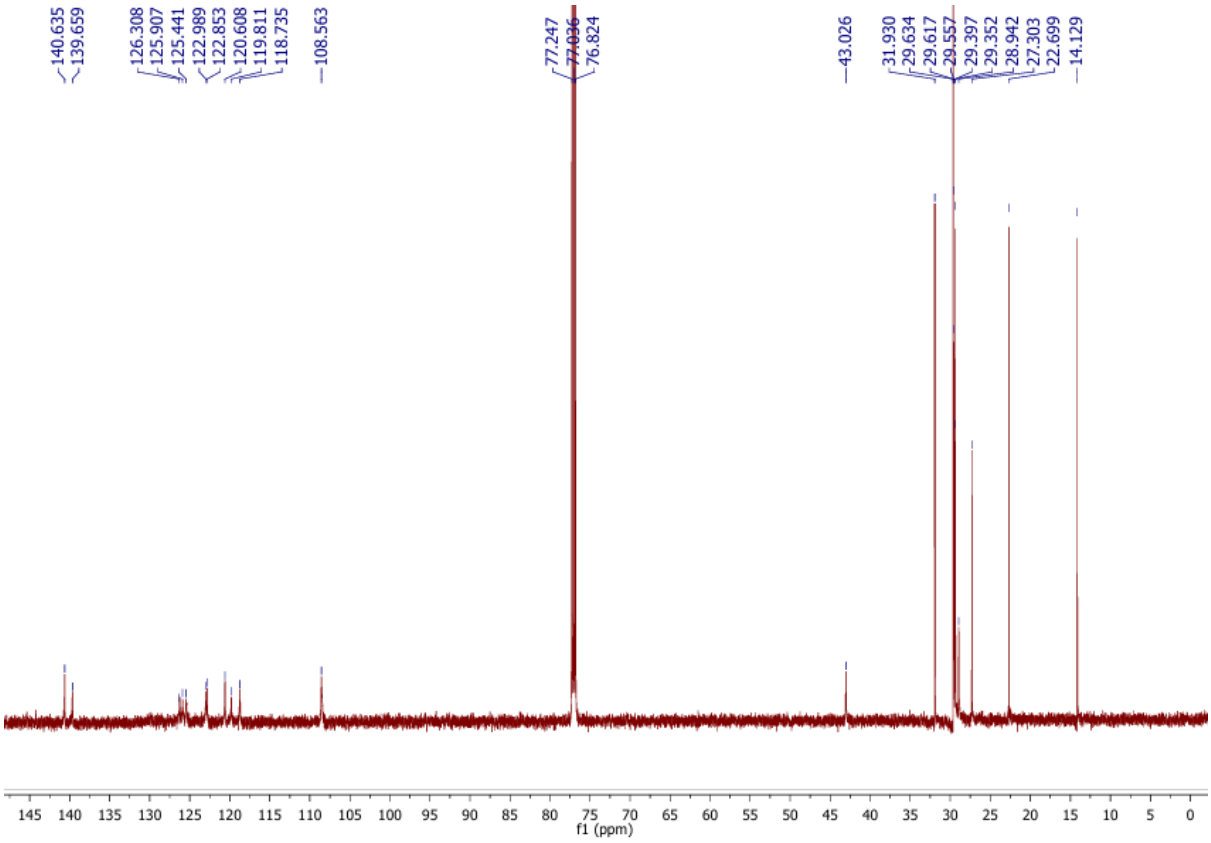

Figure S4 ^{13}C NMR (150 MHz) spectra of **CZDIM** in $CDCl_3$.

4. MALDI-TOF mass spectrum

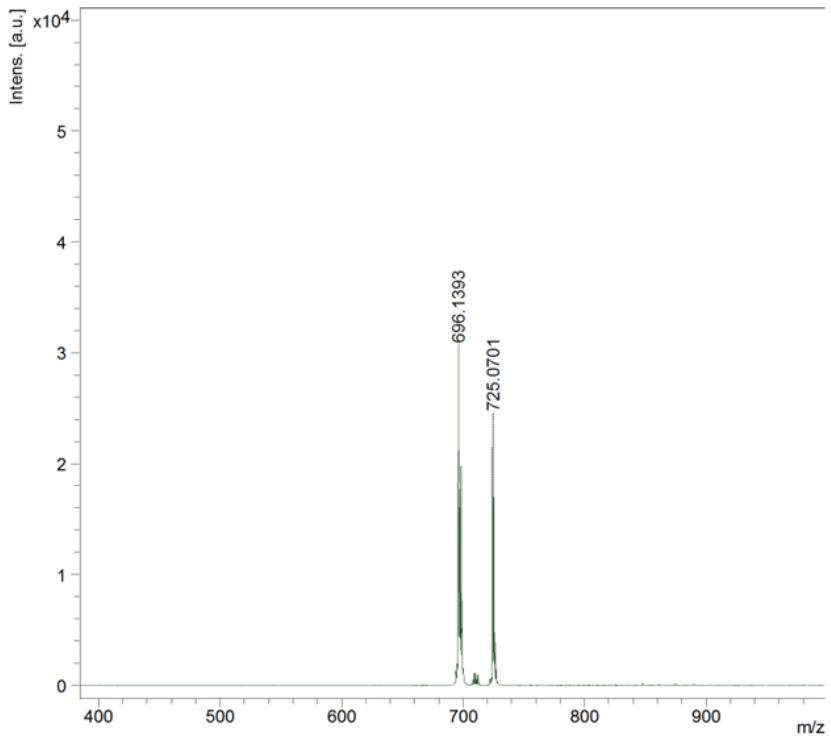

Figure S5 MALDI-TOF mass spectrum of compound **3**.

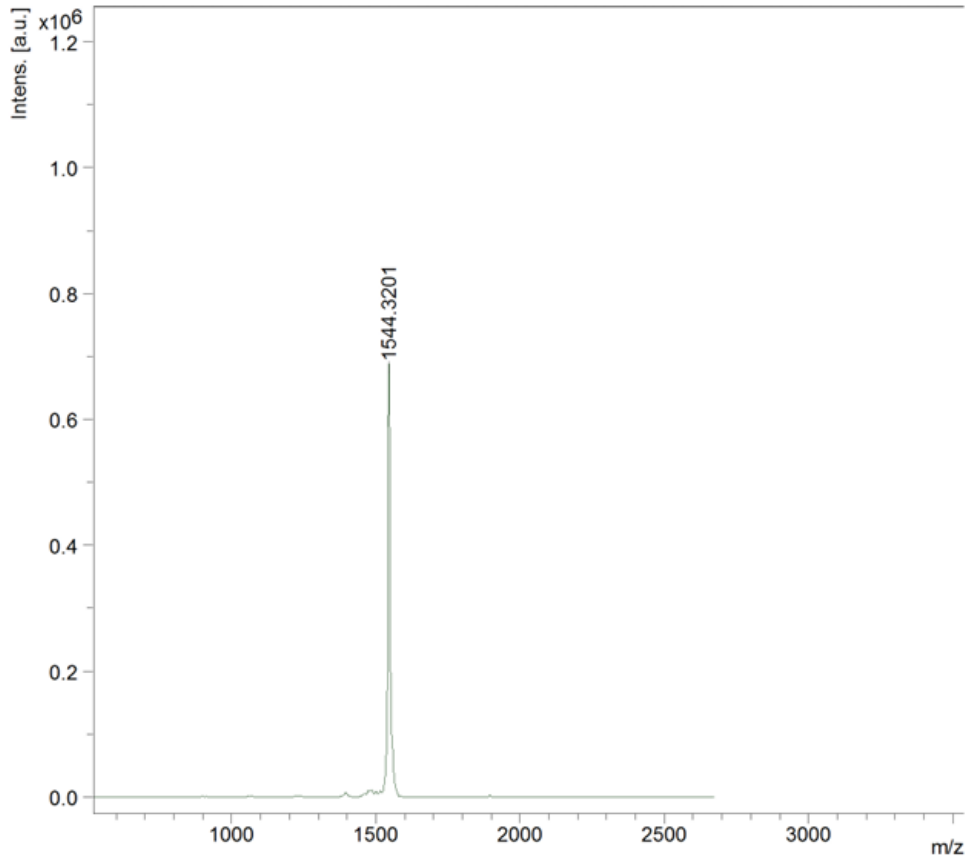

Figure S6 MALDI-TOF mass spectrum of **CZDIM**.

5. Infrared spectra

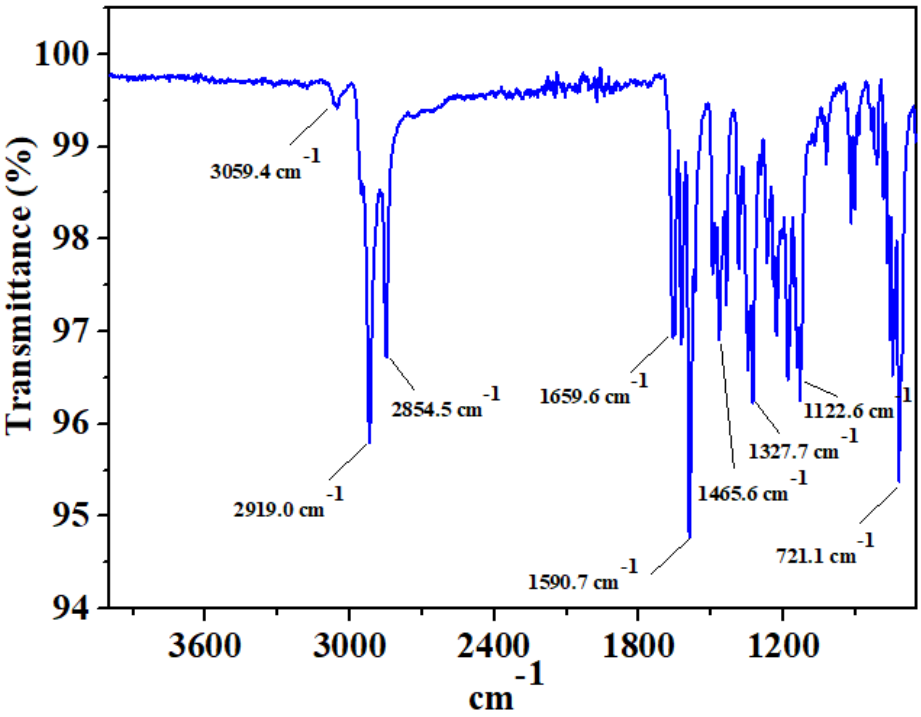

Figure S7 IR spectrum of compound **3**.

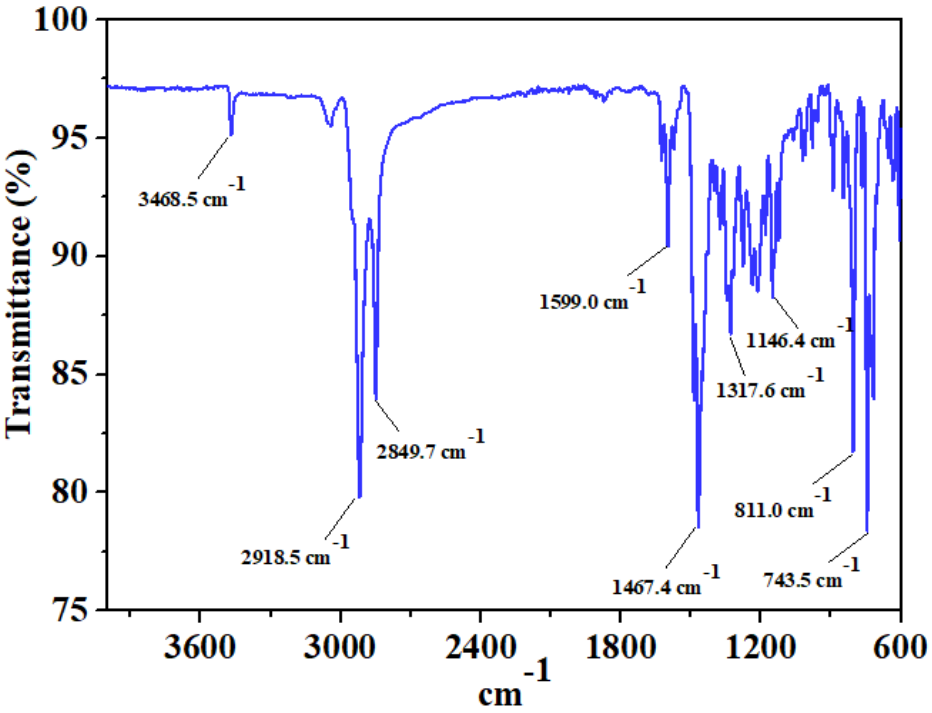

Figure S8 IR spectrum of **CZDIM**.

6. Thermogravimetric analysis and Differential scanning calorimetry

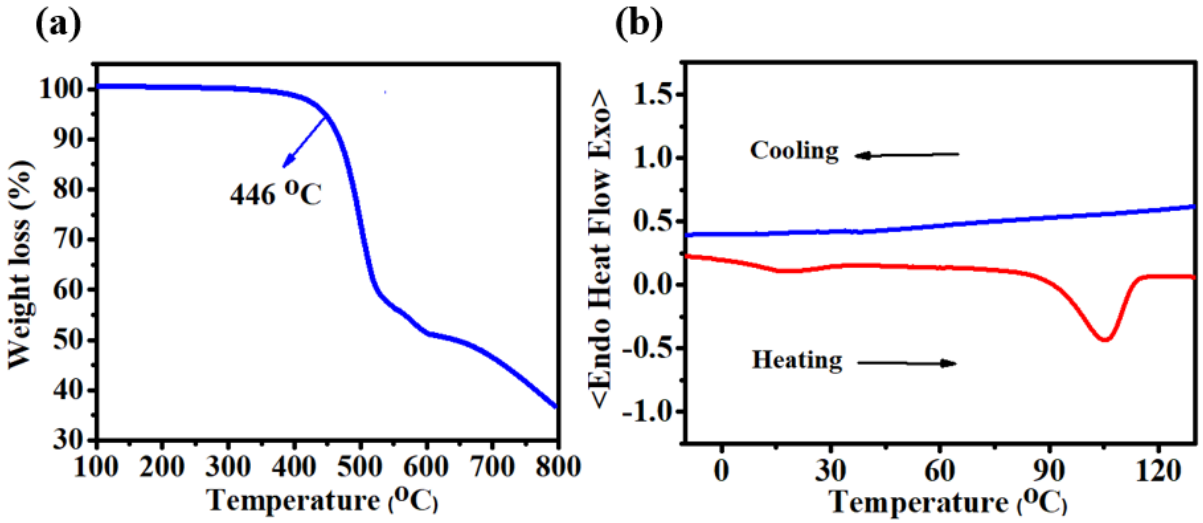

Figure S9 (a) TGA plot of compound **CZDIM** (heating rate of 10 °C/min, Nitrogen atmosphere); (b) DSC thermogram obtained for **CZDIM** for the first cooling (blue trace) and first heating (red trace) taken at 5 °C/min.

7. Gel properties

Table S1: Gelation test results of compound **CZDIM.**

Compound[a]	Hexane	Toluene	Ethyl acetate	DMF	1,4-dioxane	Decane	Ethanol	DMSO
CZDIM	PS	S	S	PS	G	PS	PS	S
[a] PS = partial soluble, S = soluble, G = stable gel at room temperature.								

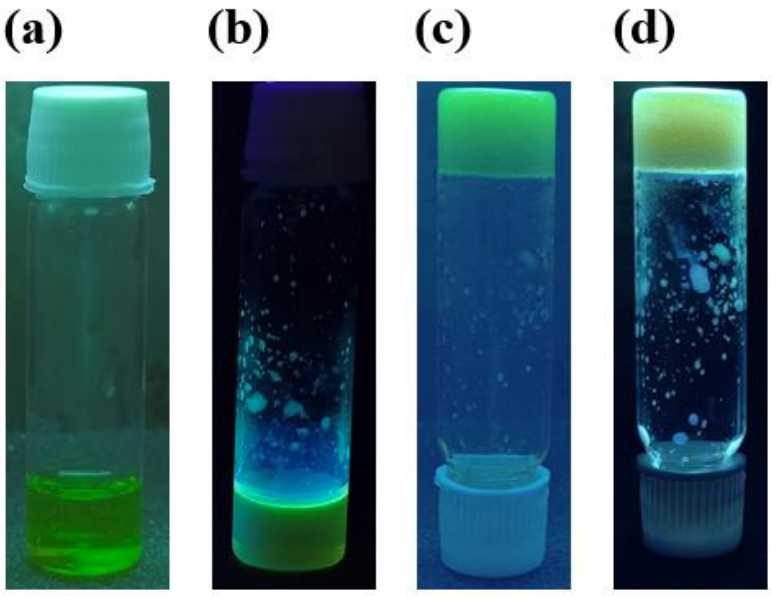

Figure S10 Photographs of the solution and gels prepared with **CZDIM** in 1,4-dioxane (1 wt%) (a, c) without irradiation; (b, d) under irradiation with 365 nm light.

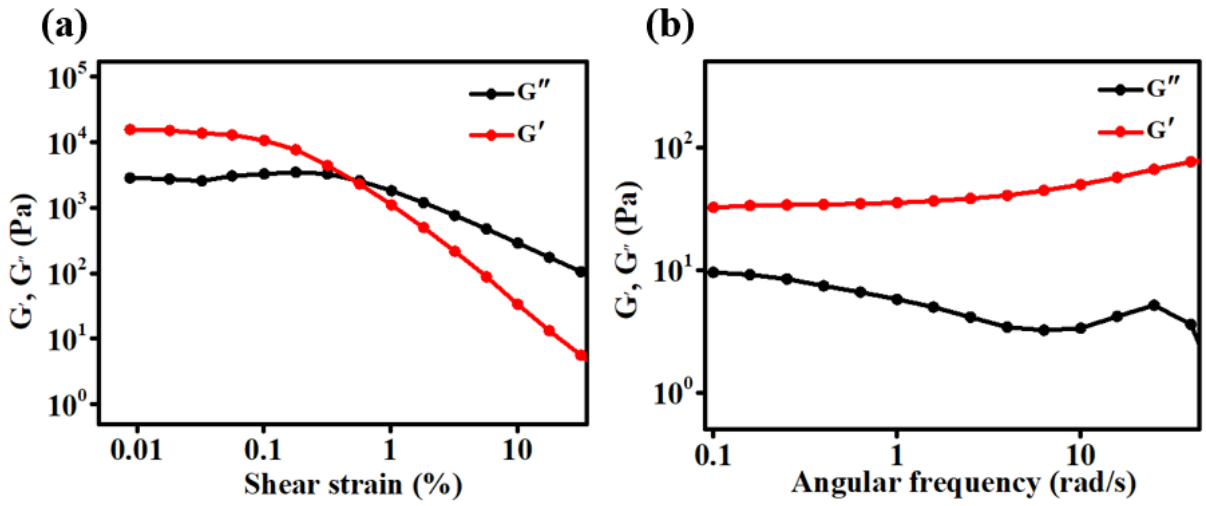

Figure S11 (a) Amplitude and (b) frequency sweep experiments of compound **CZDIM** gel in 1,4-dioxane**.**

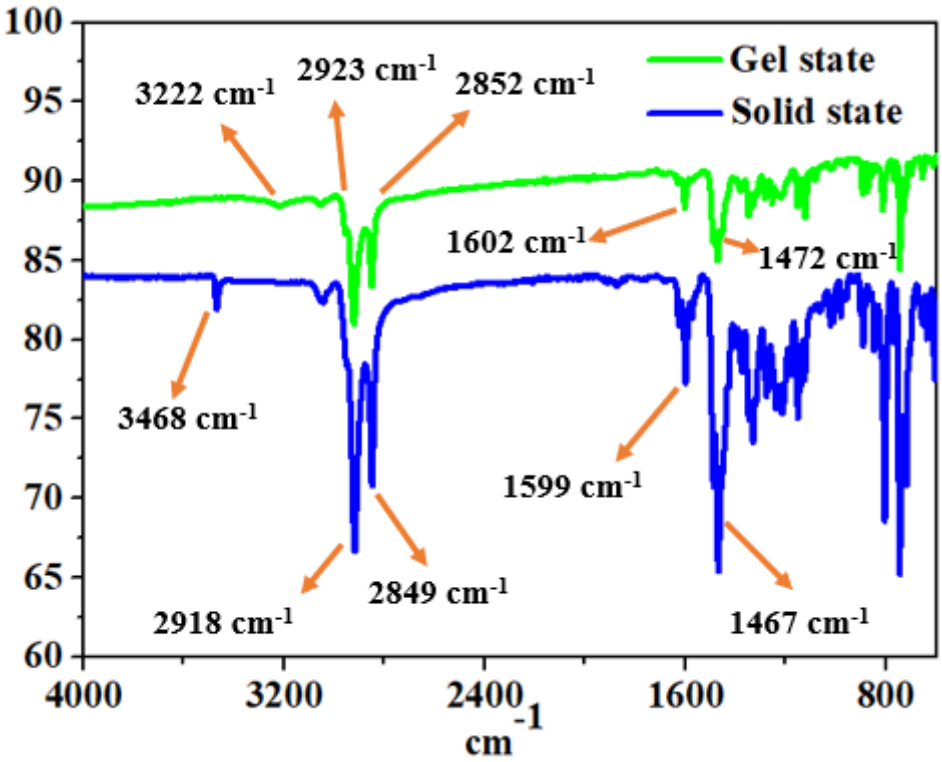

Figure S12 FT-IR spectra of compound **CZDIM** in solid state (blue) and gel state (green) made from 1,4-dioxane (1 wt%).

8. Photophysical properties

Stock solution preparation

The **CZDIM** stock solution (10 mM) was prepared in DMSO. The stock solution of the other analyte was prepared in DI Water.

Detection limit

The detection limit was evaluated based on the fluorescence titration changes. **CZDIM** fluorescence emission spectrum was computed ten times, and the standard deviation of the blank measurement was obtained. The fluorescence emission at 475 nm was plotted as a function of the concentration of BSA to determine the slope. The detection limits were calculated using the following equation:

$$\frac{3\sigma}{K} = Detection\ Limit$$

Where σ is the standard deviation of blank measurement, and K is the slope between the fluorescence emission intensity versus [BSA].

Estimation of the apparent binding constant

CZDIM was titrated with varying concentrations of BSA. The apparent binding constant for forming the **CZDIM**+BSA complex was assessed utilizing the Benesi−Hildebrand (B−H) plot (Equation 1).

$$\frac{1}{K(I_{max}-I_0)C} + \frac{1}{I_{max}-I_0} = \frac{1}{I-I_0} \text{.....(1)}$$

I_0 is the emission intensity of the complex at maximum (λ = 475 nm), and I is the recorded emission intensity at that particular wavelength in the presence of a specific concentration of the analyte (C). I_{max} is the maximum emission intensity value obtained at λ = 475 nm during titration with varying analyte concentrations. K is the apparent binding constant (M^{-1}) and was determined from the linear plot's slope.

Calculation of Förster critical radius (R_0)

The Förster's distance or critical distance R_0 is the characteristic distance at which the efficiency of energy transfer is 50%. The magnitude of R_0 is dependent on the spectral properties of the donor and the acceptor molecules. If the wavelength λ is expressed in nanometers, then J(λ) is in units of M^{-1} cm^{-1} nm^4 and the Forster distance, R_0 in angstroms (Å), is expressed as follows

$R_0 = 0.2108\ [\ k^2 n^{-4} \varphi_D J_{\mathbf{CZDIM}}]^{1/6}$ (in Å)

K^2 is the orientation factor for the emission and absorption dipoles, and its value depends on their relative orientation. n is the refractive index of the medium, and Φ_D is the quantum yield

of the donor. J(λ) is the overlap integral of the fluorescence emission spectrum of the donor and the absorption spectrum of the acceptor.

$J_{CZDIM} = \int_0^\infty I_D(\lambda)\varepsilon_A(\lambda)\lambda^4\, d\lambda$

J_{CZDIM} expresses the degree of spectral overlap between the donor emission and the acceptor absorption, where $I_D(\lambda)$ is the donor-normalized fluorescence emission spectrum, $\varepsilon_A(\lambda)$ is the acceptor molar absorption coefficient ($\varepsilon_{A\text{-}395}$ = 8253 $M^{-1}cm^{-1}$), and λ (475 nm) is the wavelength. In current experimental conditions, for this system, the J(λ) was calculated to be 5.07 x 10^{13} $M^{-1}cm^{-1}nm^4$. The Förster distance (R_0) has been calculated assuming random orientation of the donor and acceptor molecules, taking K^2 = 2/3 (for common organic fluorophores, provided that both partners are freely moveable and thus randomly oriented), n =1.33 (water), and determined Φ_D =0.13[S4,S5]

For **CZDIM** (acceptor) and BSA (donor) in the current experimental situation, by using the commercial software Origin 8.0 as the integral tool, we calculated R_0 =29.3 Å. Energy transfer will be effective for 14.4 Å≤ d ≤ 43.2 Å (R_0 ± 50% R_0)

r is the apparent distance between the donor and the acceptor, which is directly related to the experimental FRET efficiency $\langle E \rangle$ that is averaged over all sampled donor-acceptor distances R_0, but it is not a physical distance. *R* is the real distance between the center points (mean positions) of the accessible volumes and deviates from $R_{\langle E \rangle}$ because of the different averaging in distance and efficiency space. *R* cannot be measured directly but is important, for example, for mapping the physical distances required for structural modelling.

The energy transfer data were obtained by measuring the change in acceptor fluorescence. The acceptor fluorescence intensity (F_D) was measured in the absence and presence (F_A) of donor. The efficiency of energy transfer (*E*) was calculated using[S6]

$E=1 - \frac{FA}{FD}$

$E=1 - \frac{103480}{2927500} = 0.96$

$E=1 - \frac{FA}{FD} = \frac{R_0^6}{R_0^6+r^6}$

$0.96 = \frac{29.3^6}{29.3^6 + r^6}$

r = 16.85 Å

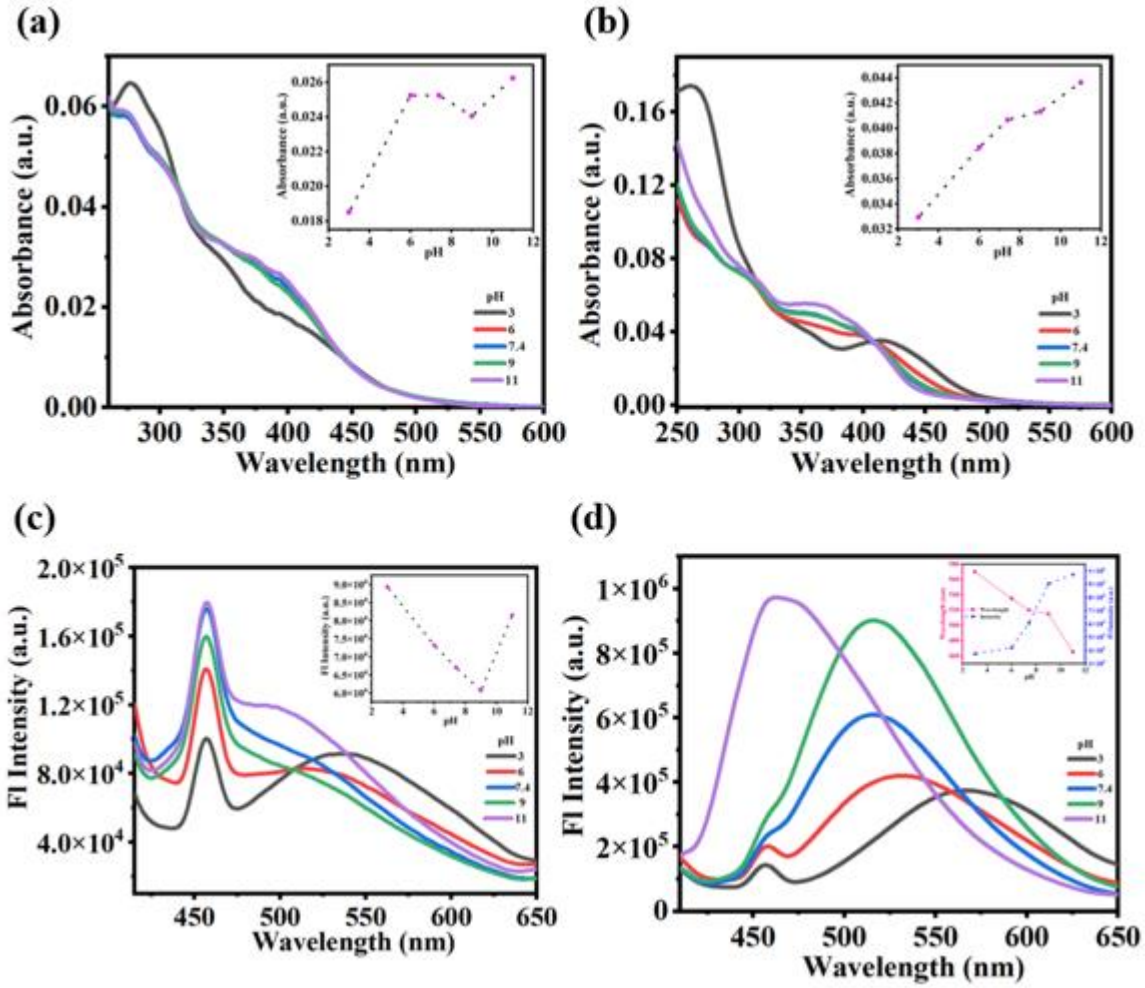

Figure S13 pH-dependent UV/Vis absorption when changed from 3 to 11 (a) at 0.25 μM below CAC, (b) 2 μM above CAC [Inset: dependence of PL Absorbance on pH]; PL spectra when pH is switched between 3 and 11 (c) at 0.25 μM below CAC, (d) 2 μM above CAC [Insert: dependence of PL intensity on pH].

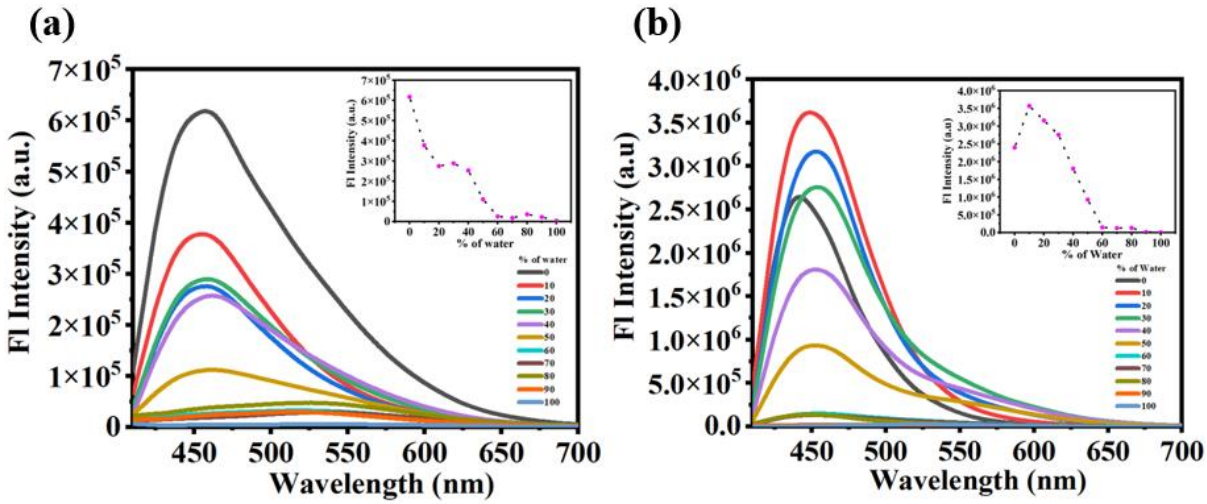

Figure S14 PL spectra of **CZDIM** in THF/water mixtures with different volume fractions of water (a) at 0.25 μM below CAC, (b) 2 μM above CAC [Inset shows the relationship between the PL peak intensity of **CZDIM** and the water fractions in THF].

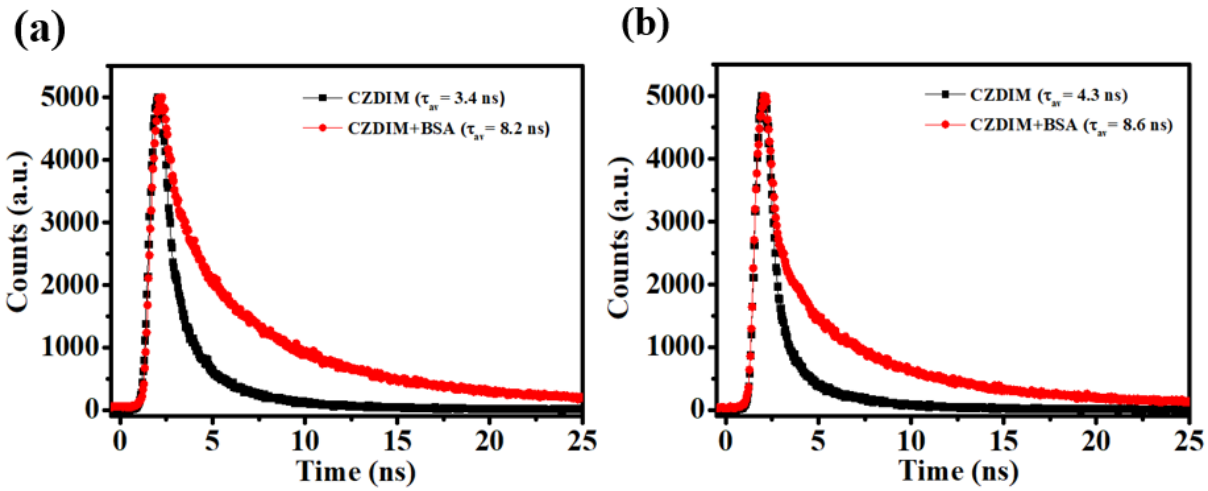

Figure S15 Time-resolved photoluminescence (TRPL) data showing change in lifetime of the fluorophore in the presence of BSA (a) at 0.25 µM below CAC, (b) 2 µM above CAC.

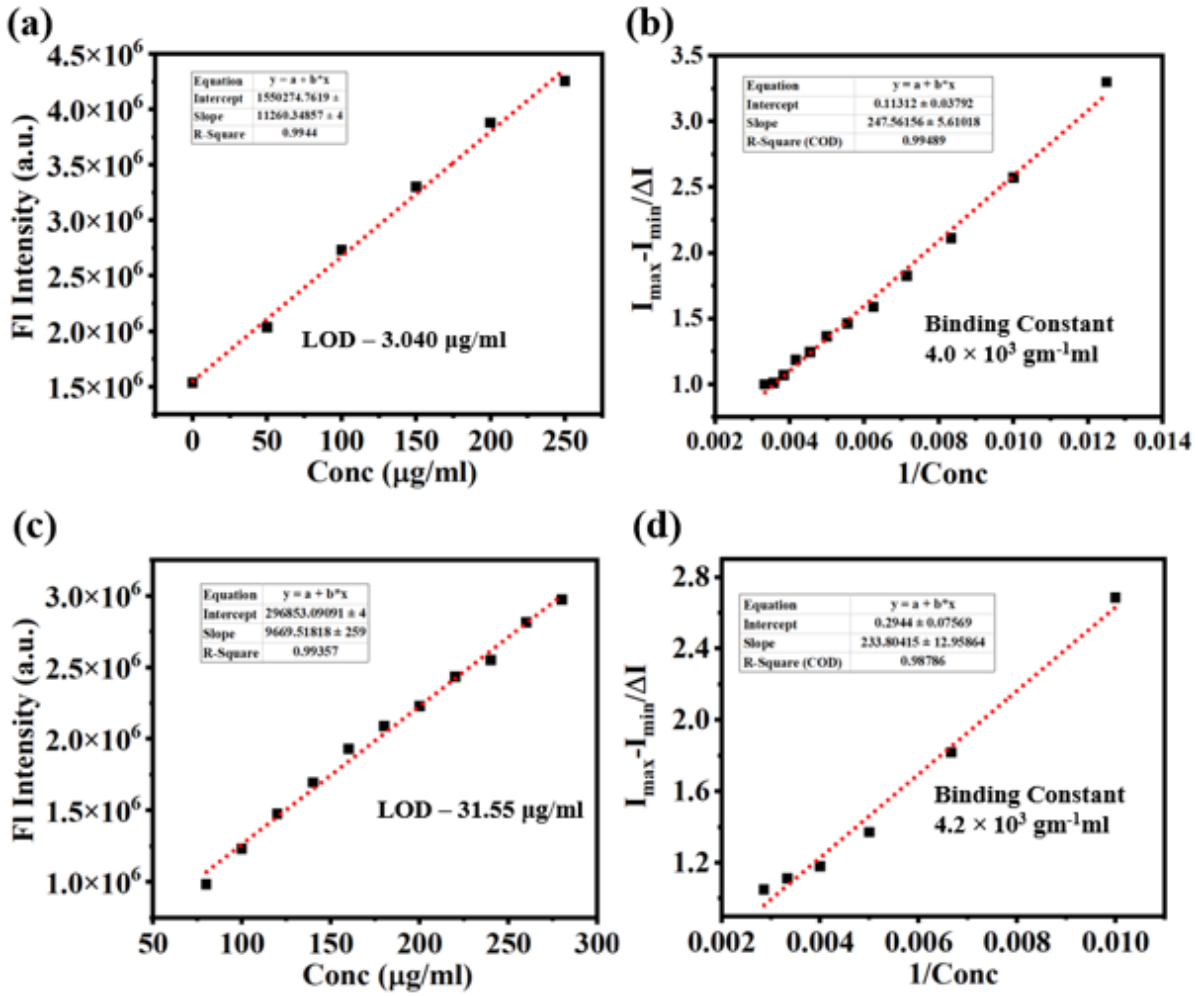

Figure S16 Linear relationship between the concentration of BSA for the detection limit (LOD) calculation (a) at 0.25 µM below CAC, (c) 2 µM above CAC; Plot for determination of binding constant for **CZDIM**-BSA (b) at 0.25 µM below CAC, (d) 2 µM above CAC.

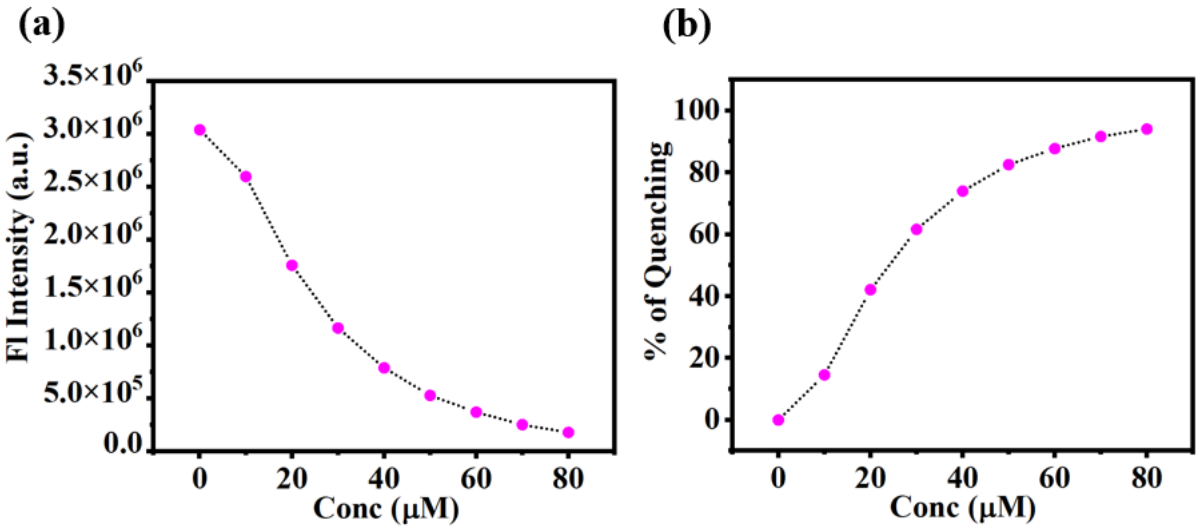

Figure S17 (a)Fluorescence intensity with respect to conc on BSA-Ibuprofen complex by **CZDIM**; (b) % of quenching of BSA-Ibuprofen complex by **CZDIM**.

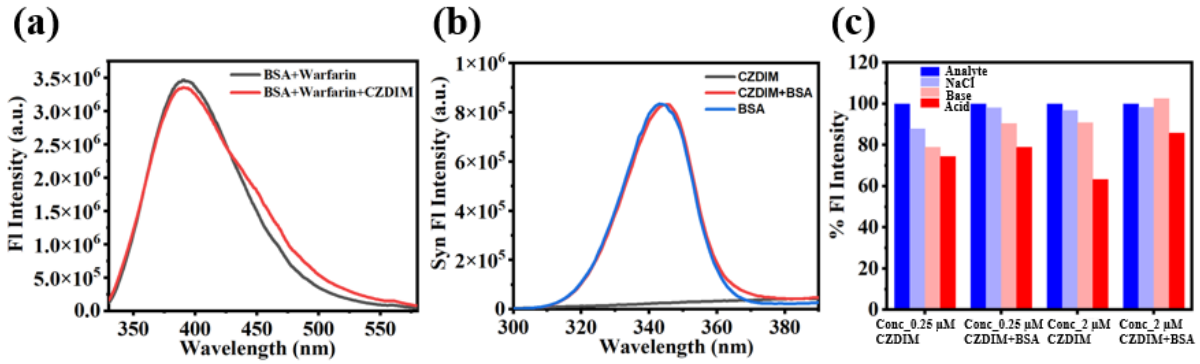

Figure S18 (a) Displacement of warfarin from BSA-warfarin complex by **CZDIM**; (b) Synchronous fluorescence spectra of BSA with various **CZDIM** {Δλ = 60 nm} for Trp; (c) Effect of acid, base, and ionic strength on **CZDIM** and **CZDIM**+BSA Complex.

Table S2: Absolute quantum yield measurement.

Sample	Scatter range (nm)	Emission range (nm)	Absorptance	Quantum yield (%)
CZDIM (0.25 µM)	389-403	427-598	0.05	0.96
CZDIM (0.25 µM) + BSA (200 µg/ml)	388-403	453-699	0.14	4.47
CZDIM (2 µM)	388-404	426-600	0.08	1.34
CZDIM (2 µM) + BSA (400 µg/ml)	390-403	452-698	0.95	7.28

Table S3: Zeta potential and particle size calculations.

Sample	Zeta Potential (mV)	Size (d.nm)	PDI
CZDIM (0.25 µM)	-0.204	143.6	0.383
BSA (200 µg/ml)	-10.6	472.5	1
CZDIM (0.25 µM) + BSA (200 µg/ml)	-7.74	179.5	0.34
CZDIM (2 µM)	-8.32	331.2	0.535

BSA (400 µg/ml)	-19.4	610.3	0.864
CZDIM (2 µM) + BSA (400 µg/ml)	-13.6	452.4	0.753

Table S4: TRPL measurement.

Sample	**τ_1 (ns)**	**τ_2 (ns)**	**B_1**	**B_2**	**τ_{av} (ns)**	**χ^2**
CZDIM (0.25 µM)	1.55	4.87	44.26	55.74	3.4	1.0119
CZDIM (0.25 µM) +BSA	3.16	10.12	27.02	72.98	8.2	1.0293
CZDIM (2 µM)	2.27	6.89	55.83	44.17	4.3	1.1673
CZDIM (2 µM) +BSA	3.57	11.21	33.81	66.19	8.6	1.0559

9. Molecular docking

The crystal structures of BSA (PDB code: 3V03) were retrieved from the protein data bank (PDB) and converted to the PDBQT format by the Autodock tool. The protein-ligand docking studies were conducted using the computational tool AutoDock Vina v.1.2.0 to calculate the binding energies of the **BSA-CZDIM** complex structure. The best pose structure was analyzed and visualized by using the Ligplot software.[S7]

10. References

S1 P. Therdkatanyuphong, P. Chasing, C. Kaiyasuan, S. Boonnab, T. Sudyoadsuk and V. Promarak, *Adv Funct Mater*, DOI:10.1002/adfm.202002481.

S2 V. K. Vishwakarma, M. R. Nagar, N. Lhouvum, J. H. Jou and A. Ammathnadu Sudhakar, *Adv Opt Mater*, DOI:10.1002/adom.202200241.

S3 V. K. Vishwakarma, M. Roy, R. Singh, D. S. Shankar Rao, R. Paily and A. Ammathnadu Sudhakar, *ACS Appl Electron Mater*, 2023, **5**, 2351–2364.

S4 L. Yuan, W. Lin, K. Zheng and S. Zhu, *Acc Chem Res*, 2013, **46**, 1462–1473.

S5 F. Gouanvé, T. Schuster, E. Allard, R. Méallet-Renault and C. Larpent, *Adv Funct Mater*, 2007, **17**, 2746–2756.

S6 B. Liu, F. Zeng, G. Wu and S. Wu, *Chemical Communications*, 2011, **47**, 8913–8915.

S7 M. Fekadu, D. Zeleke, B. Abdi, A. Guttula, R. Eswaramoorthy and Y. Melaku, *BMC Chem*, DOI:10.1186/s13065-022-00795-0.